第 33 卷第 12 期
2017 年 12 月

无 机 化 学 学 报
CHINESE JOURNAL OF INORGANIC CHEMISTRY

Vol.33 No.12
2322-2328

由联苯四羧酸配体构筑的一维锰(Ⅱ)和二维铜(Ⅱ)配位聚合物的合成、晶体结构及磁性质

陈金伟[1] 温炳松[2] 曹芳利[2] 邱文达[3] 黎 彧*,[3] 成晓玲*,[2]

([1]广东轻工职业技术学院轻化工技术学院,广州 510300)

([2]广东工业大学轻工化工学院,广州 510006)

([3]广东轻工职业技术学院生态环境技术学院,广州 510300)

摘要:采用水热方法,用 2 种联苯四羧酸配体(2,4-H_4bpta 和 3,5-H_4bpta)和 4,4′-联吡啶(4,4′-bipy)或 2,2′-联吡啶(2,2′-bipy)分别与 $MnCl_2·4H_2O$ 和 $CuCl_2·H_2O$ 反应,合成了一个具有一维双螺旋链结构的配位聚合物$[Mn(\mu_3\text{-}2,4\text{-}H_2bpta)(4,4'\text{-}bipy)_2]_n$ (**1**)和一个二维层状配位聚合物$\{[Cu(\mu_4\text{-}3,5\text{-}bpta)_{0.5}(2,2'\text{-}bipy)(H_2O)]·H_2O\}_n$ (**2**),并对其结构和磁性质进行了研究。结构分析结果表明 2 个配合物分别属于单斜晶系,$P2_1/c$ 和 $C2/c$ 空间群。配合物 **1** 具有一维双螺旋链结构,而且这些一维链通过 O–H…N 氢键作用进一步形成了二维超分子网络。而配合物 **2** 具有二维层状结构。研究表明,配合物 **1** 中相邻锰离子间存在铁磁相互作用。

关键词:配位聚合物;氢键;四羧酸配体;磁性

中图分类号:O614.121;O614.71+1 **文献标识码**:A **文章编号**:1001-4861(2017)12-2322-07

DOI:10.11862/CJIC.2017.229

Syntheses, Crystal Structures and Magnetic Properties of 1D Manganese (Ⅱ) and 2D Copper(Ⅱ) Coordination Polymers Constructed from Biphenyl Tetracarboxylic Acid

CHEN Jin-Wei[1] WEN Bing-Song[2] CAO Fang-Li[2] QIU Wen-Da[3] LI Yu*,[3] CHEN Xiao-Ling*,[2]

([1]*School of Light Chemical Engineering, Guangdong Industry Polytechnic, Guangzhou* 510300, *China*)

([2]*School of Chemical Engineering and Light Industry, Guangdong University of Techlonogy, Guangzhou* 510006, *China*)

([3]*School of Eco-Environmental Engineering, Guangdong Industry Polytechnic, Guangzhou* 510300, *China*)

Abstract: One-dimensional manganese(Ⅱ) and two-dimensional copper(Ⅱ) coordination polymers, namely $[Mn(\mu_3\text{-}2,4\text{-}H_2bpta)(4,4'\text{-}bipy)_2]_n$ (**1**) and $\{[Cu(\mu_4\text{-}3,5\text{-}bpta)_{0.5}(2,2'\text{-}bipy)(H_2O)]·H_2O\}_n$ (**2**), have been constructed hydrothermally using 2,4-H_4bpta (2,4-H_4bpta=biphenyl-2,2′,4,4′-tetracarboxylic acid), 3,5-H_4bpta (3,5-H_4bpta=biphenyl-3,3′,5,5′-tetracarboxylic acid), 4,4′-bipy (4,4′-bipy=4,4′-bipyridine) or 2,2′-bipy (2,2′-bipy=2,2′-bipyridine), and manganese or copper chlorides. Single-crystal X-ray diffraction analyses reveal that the two complexes crystallize in the monoclinic system, space group $P2_1/c$ or $C2/c$. In complex **1**, the carboxylate groups of 2,4-H_2bpta^{2-} ligands bridge alternately neighboring Mn(Ⅱ) ions to form a double-helix chain. Adjacent chains are assembled to a 2D supramolecular network through O–H…N hydrogen bond. Complex **2** shows a 2D sheet. Magnetic studies for complex **1** demonstrate a ferromagnetic coupling between the adjacent Mn(Ⅱ) centers. CCDC: 1560401, **1**; 1560402, **2**.

Keywords: coordination polymer; hydrogen bonding; tetracarboxylic acid; magnetic properties

收稿日期:2017-07-06。收修改稿日期:2017-08-23。

广东省高等职业院校珠江学者岗位计划(2015)、广东省自然科学基金(No.2016A030313761)、广东轻院珠江学者人才类项目(No.RC2015-001)、生物无机与合成化学教育部重点实验室开放基金(2016)和教育部职业教育高分子专业教学资源库项目(2015-17)资助。

*通信联系人。E-mail:liyuletter@163.com,ggcxl@163.com

In recent years, a high interest has been focused on the design and construction of the coordination polymers due to their potential applications, architectures, and topologies[1-5]. Many factors such as the coordination requirements of the metal centers, the structural characteristics of the ligand, the solvent system, and pH value can play the key role in the construction of the coordination networks[6-12]. The selection of the special ligands is very important in the construction of these coordination polymers.

Multi-carboxylate biphenyl ligands have been certified to be of great significance as constructors due to their strong coordination abilities in various modes, which could satisfy different geometric requirements of metal centers[8-17]. In order to extend our research in this field, we chose two biphenyl tetracarboxylic acid ligands, biphenyl-2,2′,4,4′-tetracarboxylic acid (2,4-H_4bpta) and biphenyl-3,3′,5,5′-tetracarboxylic acid (3,5-H_4bpta) to construct novel coordination polymers. Both H_4bpta ligands possesses the following features: (1) they have four carboxyl groups that may be completely or partially deprotonated, inducing rich coordination modes and allowing interesting structures with higher dimensionalities; (2) they can act as hydrogen-bond acceptor as well as donor, depending upon the degree of deprotonation; (3) two sets of carboxyl groups separated can form different dihedral angles through the rotation of C-C single bonds; thus, it may ligate metal centers in different orientation.

Taking into account these factors, we herein report the syntheses, crystal structures, and magnetic properties of two Mn (Ⅱ) and Cu (Ⅱ) coordination polymers constructed from H_4bpta.

1 Experimental

1.1 Reagents and physical measurements

All chemicals and solvents were of AR grade and used without further purification. Carbon, hydrogen and nitrogen were determined using an Elementar Vario EL elemental analyzer. IR spectra were recorded using KBr pellets and a Bruker EQUINOX 55 spectrometer. Thermogravimetric analysis (TGA) data were collected on a LINSEIS STA PT1600 thermal analyzer with a heating rate of 10 ℃·min^{-1}. Magnetic susceptibility data were collected in the 2~300 K temperature range with a Quantum Design SQUID Magnetometer MPMS XL-7 with a field of 0.1 T. A correction was made for the diamagnetic contribution prior to data analysis.

1.2 Synthesis of [Mn(μ_3-2,4-H_2bpta)(4,4′-bipy)$_2$]$_n$ (1)

A mixture of $MnCl_2·4H_2O$ (0.040 g, 0.20 mmol), 2,4-H_4bpta (0.066 g, 0.2 mmol), 4,4′-bipy (0.031 g, 0.2 mmol), NaOH (0.016 g, 0.40 mmol), and H_2O (10 mL) was stirred at room temperature for 15 min, and then sealed in a 25 mL Teflon-lined stainless steel vessel, and heated at 160 ℃ for 3 days, followed by cooling to room temperature at a rate of 10 ℃·h^{-1}. Yellow block-shaped crystals of **1** were isolated manually, and washed with distilled water. Yield: 35% (based on 2,4-H_4bpta). Anal. Calcd. for $C_{36}H_{24}MnN_4O_8$ (%): C 62.16, H 3.48, N 8.06; Found (%): C 61.93, H 3.44, N 8.11. IR (KBr, cm^{-1}): 1 672m, 1 624w, 1 598s, 1 572s, 1 533m, 1 489w, 1 424m, 1 377w, 1 303m, 1 277w, 1 246w, 1 216w, 1 164w, 1 120w, 1 064w, 1 042w, 999w, 972w, 899w, 851w, 808m, 773w, 730w, 691w, 656w, 626w, 569w, 543w.

1.3 Synthesis of {[Cu(μ_4-3,5-bpta)$_{0.5}$(2,2′-bipy)(H_2O)]·H_2O}$_n$ (2)

The synthesis of **2** is similar with that of **1** except that $CuCl_2·H_2O$ (0.030 g, 0.20 mmol), 3,5-H_4bpta (0.033 g, 0.1 mmol), 2,2′-bipy (0.031 g, 0.2 mmol) were used instead of $MnCl_2$, 2,4-H_4bpta and 4,4′-bipy. Blue block-shaped crystals of **2** were isolated manually, and washed with distilled water. Yield: 65% (based on 3,5-H_4bpta). Anal. Calcd. for $C_{18}H_{15}CuN_2O_6$(%): C 51.61, H 3.61, N 6.69; Found(%): C 51.78, H 3.58, N 6.65. IR (KBr, cm^{-1}): 3 647w, 3 307w, 1 604w, 1 569s, 1 493w, 1 472w, 1 448w, 1 402m, 1 356s, 1 311w, 1 250w, 1 174w, 1 114w, 1 073w, 1 052w, 1 027w, 896w, 769m, 712w, 652w, 541w. The complexes are insoluble in water and common organic solvents, such as methanol, ethanol, acetone, and DMF.

1.4 Structure determinations

The data of two single crystals with dimensions of 0.20 mm×0.16 mm×0.16 mm (**1**) and 0.25 mm×0.22

mm×0.21 mm (**2**) was collected at 293(2) K on a Bruker SMART APEX Ⅱ CCD diffractometer with Mo $K\alpha$ radiation (λ=0.071 073 nm). The structures were solved by direct methods and refined by full matrix least-square on F^2 using the SHELXTL-2014 program[18]. All non-hydrogen atoms were refined anisotropically. All the hydrogen atoms (except the ones bound to water molecules) were positioned geometrically and refined using a riding model. The hydrogen atoms of water molecules were located by difference maps and constrained to ride on their parent O atoms. A summary of the crystallography data and structure refinements for **1** and **2** is given in Table 1. The selected bond lengths and angles for complexes **1** and **2** are listed in Table 2. Hydrogen bond parameters of complexes **1** and **2** are given in Table 3.

CCDC: 1560401, **1**; 1560402, **2**.

Table 1 Crystal data for complexes 1 and 2

Complex	1	2
Chemical formula	$C_{36}H_{24}MnN_4O_8$	$C_{18}H_{15}CuN_2O_6$
Molecular weight	695.53	418.86
Crystal system	Monoclinic	Monoclinic
Space group	*C*2/*c*	$P2_1/c$
a / nm	3.521 0(2)	0.783 49(6)
b / nm	0.898 36(8)	1.366 89(8)
c / nm	0.979 53(8)	1.602 21(13)
β / (°)	103.972(6)	106.526(7)
V / nm^3	3.006 7(4)	1.645(2)
D_c / (g·cm^{-3})	1.537	1.691
Z	4	4
F(000)	1 428	856
θ range for data collection / (°)	3.269~25.046	3.263~25.044
Limiting indices	$-38 \leqslant h \leqslant 41, -10 \leqslant k \leqslant 6, -11 \leqslant l \leqslant 11$	$-9 \leqslant h \leqslant 4, -15 \leqslant k \leqslant 16, -16 \leqslant l \leqslant 19$
Reflections collected, unique (R_{int})	9 038, 2 666 (0.058 3)	5 782, 2 913 (0.067 2)
μ / mm^{-1}	0.504	1.369
Data, restraint, parameter	2 666, 0, 222	2 913, 0, 244
Goodness-of-fit on F^2	1.070	1.133
Final *R* indices R_1, wR_2 [$I \geqslant 2\sigma(I)$]	0.049 1, 0.091 4	0.062 4, 0.099 7
R indices R_1, wR_2 (all data)	0.075 4, 0.102 7	0.105 0, 0.120 4
Largest diff. peak and hole / (e·nm^{-3})	380 and −270	540 and −590

Table 2 Selected bond distances (nm) and bond angles (°) for complexes 1 and 2

1					
Mn(1)-O(1)	0.215 5(2)	Mn(1)-O(1)A	0.215 5(2)	Mn(1)-O(2)B	0.218 2(2)
Mn(1)-O(2)C	0.218 2(2)	Mn(1)-N(1)	0.231 2(2)	Mn(1)-N(1)A	0.231 2(2)
O(1)-Mn(1)-N(1)	83.10(8)	O(1)-Mn(1)-O(1)A	92.88(12)	O(1)-Mn(1)-N(1)A	88.79(9)
O(1)-Mn(1)-O(2)B	87.08(8)	O(1)-Mn(1)-O(2)C	176.83(7)	N(1)-Mn(1)-N(1)A	168.23(14)
O(2)B-Mn(1)-N(1)	88.06(8)	O(2)C-Mn(1)-N(1)	100.07(8)	O(2)B-Mn(1)-O(2)C	93.14(11)
2					
Cu(1)-O(2)	0.195 1(4)	Cu(1)-O(5)	0.198 4(3)	Cu(1)-O(3)A	0.228 8(3)
Cu(1)-N(1)	0.199 2(5)	Cu(1)-N(2)	0.200 1(5)		

Continued Table 2

O(2)-Cu(1)-O(5)	95.18(15)	O(2)-Cu(1)-N(1)	90.74(17)	O(2)-Cu(1)-N(2)	167.50(18)
O(2)-Cu(1)-O(3)A	97.12(15)	O(5)-Cu(1)-N(1)	169.65(18)	O(5)-Cu(1)-N(2)	92.07(18)
O(3)A-Cu(1)-O(5)	90.63(14)	N(1)-Cu(1)-N(2)	80.67(19)	O(3)A-Cu(1)-N(1)	97.07(15)
O(3)A-Cu(1)-N(2)	92.96(16)				

Symmetry codes: A: $-x$, y, $-z+1/2$; B: $-x$, $-y+1$, $-z+1$; C: x, $-y+1/2$, $z-1/2$ for **1**; A: $-x+2$, $y+1/2$, $-z+1/2$ for **2**.

Table 3　Hydrogen bond parameters of complexes 1 and 2

D–H···A	d(D-H) / nm	d(H···A) / nm	d(D···A) / nm	∠DHA / (°)
		1		
O(4)–H(1)···N(2)A	0.082	0.185	0.265 9	169.0
		2		
O(5)–H(1W)···O(1)	0.079	0.187	0.260 1	154.0
O(6)–H(3W)···O(3)A	0.079	0.210	0.286 8	164.0

Symmetry codes: A: $-x+1/2$, $-y+1/2$, $-z+1$ for **1**; A: $-x+2$, $y+21$, $-z+1/2$ for **2**.

2　Results and discussion

2.1　Description of the structure

2.1.1　[Mn(μ_3-2,4-H_2bpta)(4,4′-bipy)$_2$]$_n$ (**1**)

Single-crystal X-ray diffraction analysis reveals that complex **1** crystallizes in the monoclinic space group *C*2/*c*. Its asymmetric unit contains one crystallographically unique Mn(Ⅱ) ion (half occupancy), a half of μ_3-2,4-H_2bpta^{2-} block and one 4,4′-bipy moiety. As depicted in Fig.1, the six-coordinated Mn1 atom displays a distorted octahedral {MnN_2O_4} geometry filled by four O atoms from four different μ_3-2,4-H_2bpta^{2-} blocks and two N atoms from two 4,4′-bipy ligands. The lengths of the Mn-O bonds range from 0.215 5(2) to 0.218 2(2) nm, whereas the Mn-N distances are 0.231 2(2) nm; these bonding parameters are comparable to those found in other reported Mn(Ⅱ) complexes[8,13-14]. In **1**, the 2,4-H_2bpta^{2-} ligand acts as a μ_3-linker (mode Ⅰ, Scheme 1), in which two deprotonated carboxylate groups show the μ_2-η^1:η^1 bidentate mode. The dihedral angle between two phenyl rings in the 2,4-H_2bpta^{2-} is 66.14°. The 4,4′-bipy ligand adopts a terminal coordination mode, and its pyridyl rings are not coplanar showing the dihedral angle of 20.13°. The carboxylate groups of 2,4-H_2bpta^{2-} ligands bridge alternately neighboring Mn(Ⅱ) atoms in a *syn-anti* coordination fashion to form an infinite right-handed or left-handed helical Mn-O-C-O-Mn chains with the Mn···Mn separation of 0.499 7(2) nm (Fig.2). Two types of these helical chains are interconnected to each other through the Mn(Ⅱ) centers to produce double-helix chains. These are further extended into a

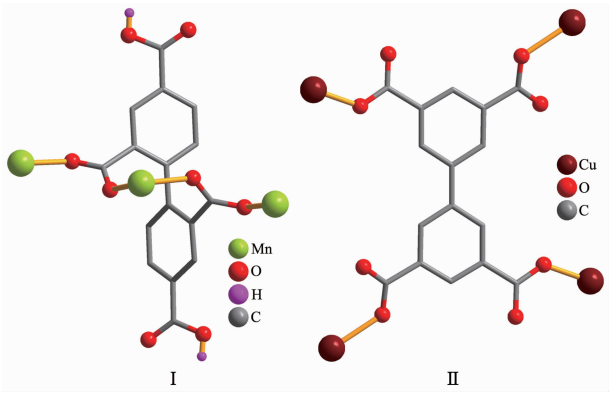

Scheme 1　Coordination modes of 2,4-H_2bpta^{2-} / 3,5-bpta^{4-} ligands in complexes **1** and **2**

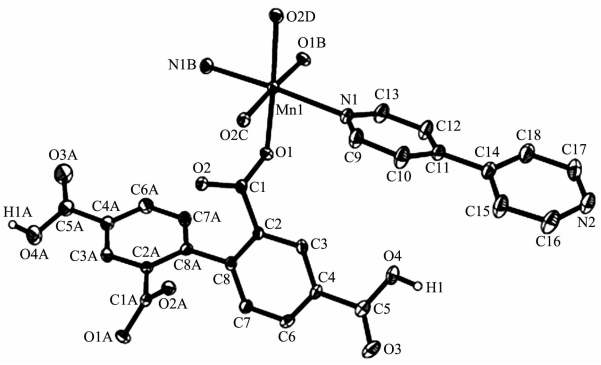

H atoms were omitted for clarity except those of COOH groups; Symmetry codes: A: $-x$, y, $-z+3/2$; B: $-x$, y, $-z+1/2$; C: $-x$, $-y+1$, $-z+1$; D: x, $-y+1$, $z-1/2$

Fig.1　Drawing of the asymmetric unit of complex **1** with 30% probability thermal ellipsoids

2D supramolecular network via the O–H···N hydrogen-bonding interactions (Fig.3 and Table 3).

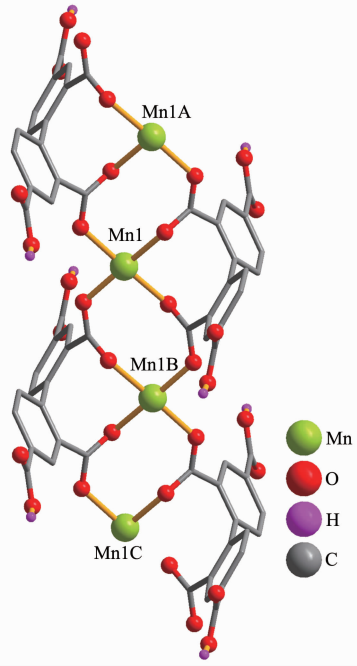

4,4′-bipy ligands are omitted for clarity; Symmetry codes: A: $-x$, $-y+1$, $-z+1$; B: $-x$, $-y+1$, $-z$; C: x, y, $z-1$

Fig.2 View of a 1D double-helix chain parallel to the *ac* plane

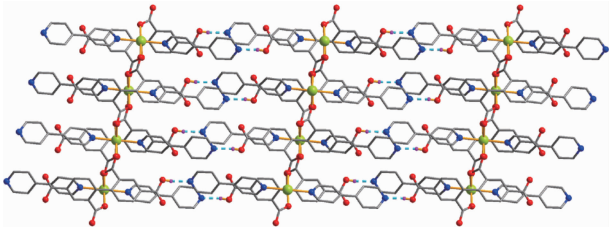

Dash lines present the H-bonds

Fig.3 Perspective of 2D supramolecular network parallel to the *ac* plane in **1**

2.1.2 $\{[Cu(\mu_4\text{-}3,5\text{-bpta})_{0.5}(2,2'\text{-bipy})(H_2O)]\cdot H_2O\}_n$ (**2**)

The asymmetric unit of **2** consists of one crystallographically distinct Cu(Ⅱ) ion, a half of one μ_4-3,5-bpta^{4-} block, one 2,2′-bipy ligand, one coordinated and one lattice water molecule. As shown in Fig.4, the Cu1 atom is five-coordinated and adopts a distorted quadrangular pyramid $\{CuN_2O_3\}$ geometry completed by two carboxylate O atoms from two distinct μ_4-3,5-bpta^{4-} blocks and one O atom from the water ligand as well as two N atoms from one 2,2′-bipy ligand. The Cu-O distances range from 0.195 1(4) to 0.228 8(3) nm, whereas the Cu-N distances vary from 0.199 2(5) to 0.200 1(5) nm; these bonding parameters are comparable to those observed in other Cu(Ⅱ) complexes [13,16-17]. In **2**, the 3,5-bpta^{4-} block acts as a μ_4-spacer (mode Ⅱ, Scheme 1), in which all carboxylate groups exhibit the μ_1-η^1:η^0 monodentate modes. In the 3,5-bpta^{4-}, two benzene rings are coplanar. The carboxylate groups of the 3,5-bpta^{4-} ligands multiply bridge the adjacent Cu(Ⅱ) ions to form a 2D sheet (Fig.5).

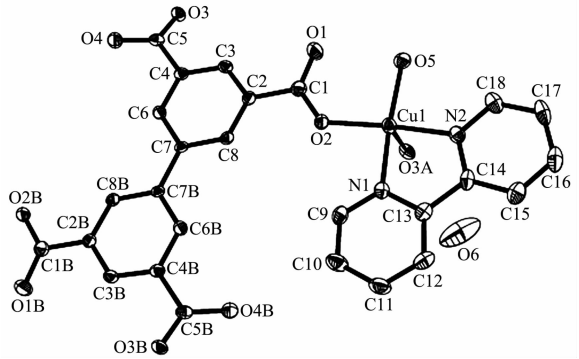

H atoms were omitted for clarity; Symmetry codes: A: $-x$, y, $-z+1/2$

Fig.4 Drawing of the asymmetric unit of complex **2** with 30% probability thermal ellipsoids

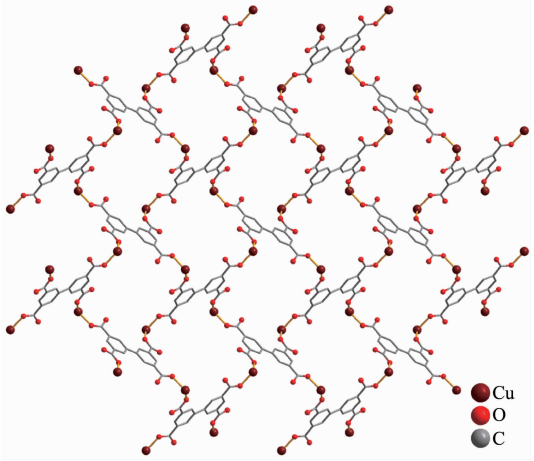

2,2′-bipy ligands were omitted for clarity

Fig.5 Two-dimensional metal-organic framework along the *a* axis in complex **2**

2.2 TGA analysis

To determine the thermal stability of complexes **1** and **2**, their thermal behaviors were investigated under nitrogen atmosphere by thermogravimetric analysis (TGA). As shown in Fig.6, The TGA curve of **1** indicates that the complex is stable up to 346 ℃, and then decompose upon further heating. The TGA curve of **2** reveals that one lattice and one coordinated water

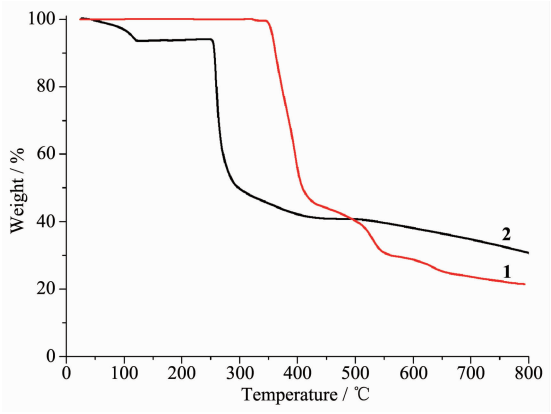

Fig.6　TGA plots of complexes **1** and **2**

molecule is released between 40 and 120 ℃ (Obsd. 8.1%; Calcd. 8.5%), and the dehydrated solid begins to decompose at 250 ℃.

2.3　Magnetic properties

Variable-temperature magnetic susceptibility studies were carried out on powder sample of complex **1** in the 2~300 K temperature range. As shown in Fig. 7, the room temperature value of $\chi_M T$ (4.41 $cm^3 \cdot mol^{-1} \cdot K$) is close to that expected for one magnetically isolated high-spin Mn(Ⅱ) ions (4.38 $cm^3 \cdot mol^{-1} \cdot K$, S=5/2, g=2.0). When the temperature is lowered, the $\chi_M T$ values increase slowly until about 50 K, then increase quickly to 7.39 $cm^3 \cdot mol^{-1} \cdot K$ at 2.0 K. Between **2** and 300 K, the magnetic susceptibilities can be fitted to the Curie-Weiss law with C=4.50 $cm^3 \cdot mol^{-1} \cdot K$ and θ=3.80 K. These results indicate a ferromagnetic interaction between the adjacent Mn(Ⅱ) centers in complex **1**. We tried to fit the magnetic data of **1** using the following expression for a 1D Mn(Ⅱ) chain[19]:

$$\chi_{chain}=[Ng^2\beta^2/(kT)](2.916\ 7+208.04x^2)(1+15.543x+2\ 707.2x^3)^{-1}$$

$$x=|J|/(kT)$$

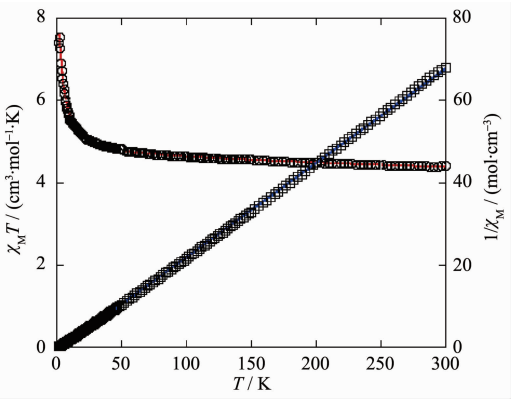

Line represents the best fit to the equations in the text and the Curie-Weiss fitting

Fig.7　Temperature dependence of $\chi_M T$ (○) and $1/\chi_M$(□) for complex **1**

Using this rough model, the susceptibilities were simulated, leading to J=+2.87 cm^{-1}, g=2.03. The positive J parameter indicates that a weak ferromagnetic exchange coupling exists between the adjacent Mn(Ⅱ) centers in **1**, which is agreement with positive θ value. According to the structure of **1** (Fig.2), there is one magnetic exchange pathway within the chain through two *syn-anti* carboxylate bridges, which could be responsible for the observed ferromagnetic exchange.

3　Conclusions

In summary, two new coordination polymers, namely $[Mn(\mu_3\text{-}2,4\text{-}H_2bpta)(4,4'\text{-}bipy)_2]_n$ (**1**) and $\{[Cu(\mu_4\text{-}3,5\text{-}bpta)_{0.5}(2,2'\text{-}bipy)(H_2O)]\cdot H_2O\}_n$ (**2**), have been synthesized under hydrothermal conditions. The complexes feature the 1D double-helix chain and 2D sheet structures, respectively. Magnetic studies show a ferromagnetic coupling between the adjacent Mn(Ⅱ) centers.

References:

[1] Catala L, Mallah T. *Acc. Chem. Res.*, **2017**,**50**:805-813
[2] He C B, Liu D M, Lin W B. *Chem. Rev.*, **2015**,**115**:11079-11108
[3] Li J R, Sculley J, Zhou H C. *Chem. Rev.*, **2012**,**112**:869-932
[4] Cui Y, Yue Y, Qian G, et al. *Chem. Rev.*, **2012**,**112**:1126-1162
[5] Kuppler R J, Timmons D. J, Fang Q R, et al. *Coord. Chem. Rev.*, **2009**,**253**:3042-3066
[6] Ji P F, Manna K, Lin Z, et al. *J. Am. Chem. Soc.*, **2016**,**138**:12234-12242
[7] Manna P, Das S K. *Cryst. Growth Des.*, **2015**,**15**:1407-1421
[8] Gu J Z, Gao Z Q, Tang Y. *Cryst. Growth Des.*, **2012**,**12**:3312-3323
[9] Gu J Z, Wu J, Lü D Y, et al. *Dalton Trans.*, **2013**,**42**:4822-4830
[10]Li Q Q, Zhang W Q, Ren C Y, et al. *CrystEngComm*, **2016**, **18**:3358-3371

[11]Huang Y Q, Chen H Y, Li Z G, et al. *Inorg. Chim. Acta*, **2017**,**466**:71-77

[12]Huang Y Q, Wan Y, Chen H Y, et al. *New J. Chem.*, **2016**, **40**:7587-7595

[13]Gu J Z, Liang X X, Cui Y H, et al. *CrystEngComm*, **2017**, **19**:117-128

[14]Li S D, Lu L P, Su F. *Chin. J. Struct. Chem.*, **2016**,**35**:1920-1928

[15]GU Jin-Zhong(顾金忠), GAO Zhu-Qing(高竹青), DOU Wei (窦伟), et al. *Chinese J. Inorg. Chem.*(无机化学学报), **2009**, **25**(5):920-923

[16]Su F, Lu L P, Feng S S, et al. *Dalton Trans.*, **2015**,**44**:7213-7222

[17]Tian H, Wang K, Jia Q X, et al. *Cryst. Growth Des.*, **2011**, **11**:5167-5170

[18]Spek A L. *Acta Crystallogr. Sect. C*, **2015**,**C71**:9-18

[19]Mahata P, Natarajan S, Panissod P, et al. *J. Am. Chem. Soc.*, **2009**,**131**:10140-10150